Science of the Total Environment 870 (2023) 161898

Contents lists available at ScienceDirect

Science of the Total Environment

journal homepage: www.elsevier.com/locate/scitotenv

Confronting turbidity, the major challenge for satellite-derived coastal bathymetry

Isabel Caballero [a,*], Richard P. Stumpf [b]

[a] Instituto de Ciencias Marinas de Andalucía (ICMAN), Consejo Superior de Investigaciones Científicas (CSIC), Avenida República Saharaui, 11519 Puerto Real, Spain
[b] National Oceanic and Atmospheric Administration (NOAA), National Centers for Coastal Ocean Science, Silver Spring, MD 20910, United States of America

HIGHLIGHTS

- The twin satellites Sentinel-2 are used for mapping shallow seabed cartography.
- Several environments are evaluated along the Caribbean and eastern coast of the USA.
- A multi-temporal compositing method automatically addresses water quality issues.
- The maximum detectable depth is defined and optically deep-water areas are removed.
- The model provides comprehensively and detailed operational bathymetric monitoring.

GRAPHICAL ABSTRACT

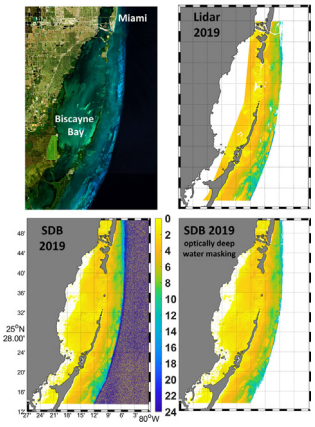

ARTICLE INFO

Editor: José Virgílio Cruz

Keywords:
Copernicus program
Remote sensing
Seabed cartography
Turbidity correction
Optically deep-water masking
Operational monitoring

ABSTRACT

Monitoring the complex seafloor morphology that drives the functioning of shallow coastal ecosystems is vital for assessing marine activities. Satellite-derived bathymetry (SDB) can provide a crucial dataset for creating the bathymetry maps needed to understand hazards and impacts produced by climate change in vulnerable coastal zones. SDB is effective in clear water, but still has limitations in application to areas with some turbidity. Here, using the twin satellites Sentinel-2A/B, we integrate water quality information from the satellite with a multi-temporal compositing method to demonstrate a potential for comprehensively operational bathymetric mapping over a range of environments. The automated compositing method diminishes the turbidity impact in addition to inferring the maximum detectable depth and removing optically deep-water areas. Examining a wide range of conditions along the Caribbean and eastern coast of the U.S. shows detailed bathymetry as deep as 30 m at 10 m spatial resolution with median errors <1 m when compared to high-resolution lidar surveys. These results demonstrate that the model adopted can provide useful bathymetry in areas that do not have consistently clear water and can be extended across multiple geographic regions and optical conditions at local, regional, and national scales.

1. Introduction

Coastal regions are strategic environments, representing an immense socio-economic and ecological value to biodiversity conservation, sustainable development, and climate change mitigation (Beck et al., 2018; Su et al., 2021). In addition, around 10 % of the world's population lives in

* Corresponding author.
E-mail address: isabel.caballero@icman.csic.es (I. Caballero).

http://dx.doi.org/10.1016/j.scitotenv.2023.161898
Received 10 October 2022; Received in revised form 18 January 2023; Accepted 25 January 2023
Available online 31 January 2023

low-elevation coastal zones, which are most vulnerable to the dynamics of natural and human-induced changes (Neumann et al., 2015; Luijendijk et al., 2018; Melet et al., 2020). Large-scale observations of critical parameters, such as shallow coastal bathymetry, are required to comprehend and predict coastal changes (Beck et al., 2018; Turner et al., 2021). Precise and up-to-date bathymetric information is basic for navigation, integrated resource management, marine spatial planning, nearshore hydrological studies, commercial and military activities, offshore engineering projects, fisheries, and aquaculture, among many other applications (Kendall et al., 2018; Cesbron et al., 2021). Furthermore, high-resolution bathymetric maps represent a crucial dataset to describe the seafloor and its benthic habitats (Hedley et al., 2018) and to understand hazards and impacts produced by climate change, sea level rise, and erosional trends at hotspots (Lin et al., 2012; Vitousek et al., 2017; Kendall et al., 2018). However, according to the International Hydrographic Organization (IHO C-55, 2021), an estimated half of the world's shallow seafloor remains unsurveyed, and available bathymetric information is frequently inadequate or decades old. Conventional surveying techniques, such as lidar on aircraft and echo sounders on ships, are constrained by environmental (waves and shallow water for shipboard, and turbidity for lidar) and logistical limitations, with practical deployment typically in relatively small areas (Cesbron et al., 2021). Mapping, charting, and change detection will benefit from the implementation of new cost-effective techniques for obtaining bathymetry at a range of scales.

In shallow coastal regions, satellites with Earth Observation (EO) capabilities are the only source of information available to complement the more restricted in situ measurements. In this sense, satellite-derived bathymetry (SDB), the determination of water depths with remote sensing, provides a potential alternative for cost-effective synoptic monitoring (Turner et al., 2021). Cesbron et al. (2021) discussed the state-of-the-art on SDB approaches and end-user requirements for many marine sectors, highlighting that integrating SDB into the bathymetry toolbox will provide the best compromise in coverage, time, and investment for generating needed bathymetric information. Publicly available, routinely sampled, and easily accessible satellite optical images have achieved a stage of maturity to support the development of SDB in the last decade (Dekker et al., 2011; Kutser et al., 2020; Turner et al., 2021). As SDB application continues to expand, defining the potential, reliability, and limitations takes on new significance. Furthermore, the Seabed 2030, a collaborative project between the Nippon Foundation of Japan and the General Bathymetric Chart of the Oceans (GEBCO), aims to bring together all available bathymetric data to produce a definitive and accessible map of the world ocean floor by 2030. Doubtless, SDB techniques can help achieving this objective by filling the GEBCO coastal database.

SDB was developed for environments such as coral atolls that have extremely clear water; as a result, SDB methods still have limitations, particularly when applied to the turbid nearshore areas found in most of the world's coastal systems (Kutser et al., 2020). Turbidity typically causes an underestimation of depths, severely affecting the performance of SDB models (Stumpf et al., 2003; Minghelli-Roman and Dupouy, 2013; Hamylton et al., 2015; Pe'eri et al., 2016; Caballero et al., 2019; Caballero and Stumpf, 2020a,b; Casal et al., 2020). Multi-scene approaches overcoming present limitations in SDB applications have been proposed as a solution to achieving more accurate and reliable bathymetry (Traganos et al., 2018; Caballero and Stumpf, 2020a,b; Kutser et al., 2020; Lebrec et al., 2021). In addition, SDB is not effective in optically deep waters (ODW), those waters where a signal is not returned from the bottom due to the combination of turbidity and depth (Dekker et al., 2011). Typically, visual interpretation and manual selection are used to select optimal imagery for SDB purposes, but these procedures are labor-intensive and subjective. Therefore, to ensure excellent accuracy and stability, especially over moderately turbid environments, automated correction for atmospheric and turbidity effects (Kutser et al., 2020; Ashphaq et al., 2021¸ Cesbron et al., 2021) and identification of ODW (Cao et al., 2020; Lee et al., 2021; Lee et al., 2022) are essential steps.

The Multispectral Instrument (MSI) on the Sentinel-2A/B twin satellite mission of the European Commission's EO Copernicus program is now a resource that provides routine and frequent global coverage with free and open-data access policy to all users. The Sentinel-2 constellation currently benefits mapping services and applications such as agriculture, land management, forestry, risk mapping, disaster control, and security issues (Osadchiev, 2018; Lacroix et al., 2020; Plank et al., 2020; Hunt et al., 2021; Normandeau et al., 2021; Rajendran et al., 2021; van Zelst et al., 2021). Sentinel-2 MSI also provides the ability to efficiently and repeatedly monitor water bodies with high temporal (5-day revisit at the equator) and spatial (10 m) resolutions, substantially enhancing data collection (Bergsma and Almar, 2020¸ Biermann et al., 2020; Caballero et al., 2020; Cira et al., 2022). Because the decametric Copernicus Sentinel-2 time series is freely available and routinely acquired at high frequency, it is an optimal source of data-compared to commercial metric or sub-metric very high resolution (VHR) imagery-for developing operational SDB monitoring programs at regional or national scales. This is particularly the case in dealing with transient conditions such as turbidity, which requires multi-temporal imagery.

In this study, we examined the effectiveness of an innovative multi-temporal composite algorithm implemented with the MSI imagery (Caballero and Stumpf, 2020a,b) to produce accurate water depths over several areas having differing turbidity and other environmental conditions. We further developed and applied a procedure to infer the maximum detectable depth to mask out ODW. The main objective was to demonstrate that this semi-automated approach can be applied in tropical and mid-latitude areas having different atmospheric conditions, water quality, and seabed habitats along the eastern coast of the U.S and the Caribbean (Figs. 1 and 2). High-resolution lidar surveys were used for SDB skill assessment, model accuracy, and consistency verification. We show the SDB algorithm's strength, especially the multi-scene compositing process that takes care of many issues, overcoming the challenges faced by the traditional single-scene models. With the advancement of satellite technologies and improved adaptability of SDB in heterogeneous environments, as exhibited in this study, we advocate the generation of future bathymetric maps of the world's coastal areas with full coverage employing the Sentinel-2 twin satellite mission.

2. Methods

2.1. Satellite imagery

The Sentinel-2A/B twin mission was utilized for SDB due to the open data access policy and high spatial resolution (10-20-60 m). The European Commission and the European Space Agency (ESA), in the frame of the Copernicus program, developed this optical constellation to support operational requirements for land, lakes, and coastal waters. The two satellites have a global revisit frequency of five days at the Equator. Details on the temporal, spectral, spatial, and radiometric features of sensors can be found in the ESA User Handbook (ESA, 2015). The stated quality standards for the absolute geo-location of the Sentinel-2 scenes (two pixels, 20 m) are within the ESA requirements (ESA, 2017). The scenes covering the seven study regions were downloaded from the ONDA DIAS (https://www.onda-dias.eu/cms/es/) corresponding to Puerto Rico (tile T19QGV), Florida Keys (T17RMH), Miami (tile T17RNJ), Cape Lookout (T18SUD), Hatteras Inlet (T18SVE), Nantucket (T19TCF), and Cape Cod (tile 19TDG). These images corresponded to Level-1C (L1C) radiometrically and geometrically corrected top-of-atmosphere (TOA) products. The study period was selected based on lidar collection for each site: 2018 for Puerto Rico, Nantucket, and Cape Cod, and 2019 for Keys, Miami, Cape Lookout, and Hatteras Inlet (the latter also post-dates the 2018 Hurricane Florence). The images used in this analysis were only screened for clouds over the study areas.

2.2. Atmospheric correction

The images were processed to Remote Sensing Reflectance (Rrs, sr^{-1}) with ACOLITE. This process eliminates the interference of atmospheric scattering and absorption, and sensor and environmental noise. ACOLITE,

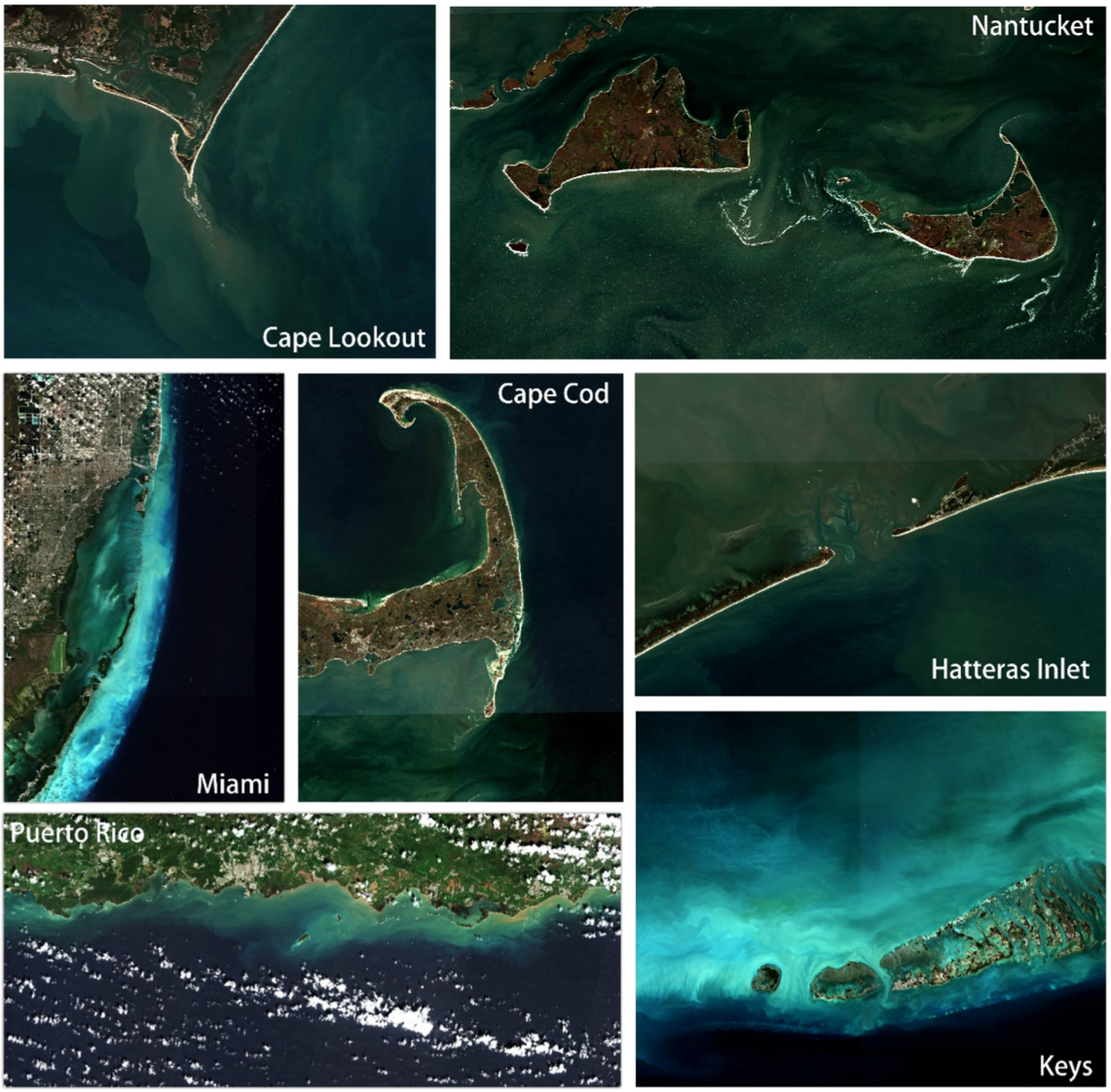

Fig. 1. Sentinel-2 true colour composite of the study regions in Puerto Rico, Florida Keys, Miami, Cape Lookout, Hatteras Inlet, Nantucket, and Cape Cod, highlighting the broad range of geography and challenging conditions of the water quality in each site.

developed by the Royal Belgian Institute of Natural Sciences (RBINS), corrects Level-1 to Level-2 data products over marine, inland, and coastal waters (Vanhellemont and Ruddick, 2016). This software incorporates an image-based model, without requiring additional in situ atmospheric datasets. The Dark Spectrum Fitting (DSF) atmospheric correction algorithm was applied (Vanhellemont and Ruddick, 2018; Vanhellemont, 2019). The notably enhanced spectral resolution of the Sentinel-2 satellites is key to obtaining good-quality products using the DSF model (Vanhellemont, 2019; Pahlevan et al., 2021). Correction of the sunglint over the surface reflectance was performed using the additional image-based sunglint correction, since, during the study period, acute sunglint effects were observed at these latitudes. The Rrs products along the visible and near-infrared (NIR) spectrum were calculated after resampling to 10 m pixel size. A further spatial filter (median filter on 3 × 3 pixel box) was applied to the corrected bands to remove noise and inter-pixel variability with minimal smoothing. Detailed information on this atmospheric and sunglint correction can be found in Caballero and Stumpf (2020b).

2.3. Bathymetric model

SDB was obtained with the extensively utilized band ratio model (Stumpf et al., 2003). Recent advancements using this SDB model were also developed, based on a semi-automated multi-scene methodology as a solution for operational bathymetric mapping over turbid regions (Caballero et al., 2020). Therefore, this multi-temporal approach was also implemented in this study to reduce the impact of turbidity by employing a compositing algorithm and to improve monitoring in very shallow water utilizing a switching algorithm. The study regions have local sources of suspended material, colored dissolved organic matter, and phytoplankton, so water quality is heterogeneous in time and space. The scenes within 3 months around the date of each lidar survey were collected. The underlying analysis uses a linear transform (Stumpf et al., 2003) of the form:

$$pSDB_{ij} = \ln\left(n\,\pi\,Rrs(\lambda_i)\right) / \ln\left(n\,\pi\,Rrs(\lambda_j)\right) \quad (1)$$

with n a constant value of 1000 and λ indicating the appropriate bands, i and j (e.g., 490, 560, 650 nm), and the depth is retrieved from an equation of the form:

$$SDB = m_1 * (pSDB - m_{offset}) \quad (2)$$

with coefficients m_1 and m_{offset} derived by tuning the SDB composited images for each site with a linear regression using ~15 calibration points obtained from NOAA chart soundings (https://www.charts.noaa.gov/)

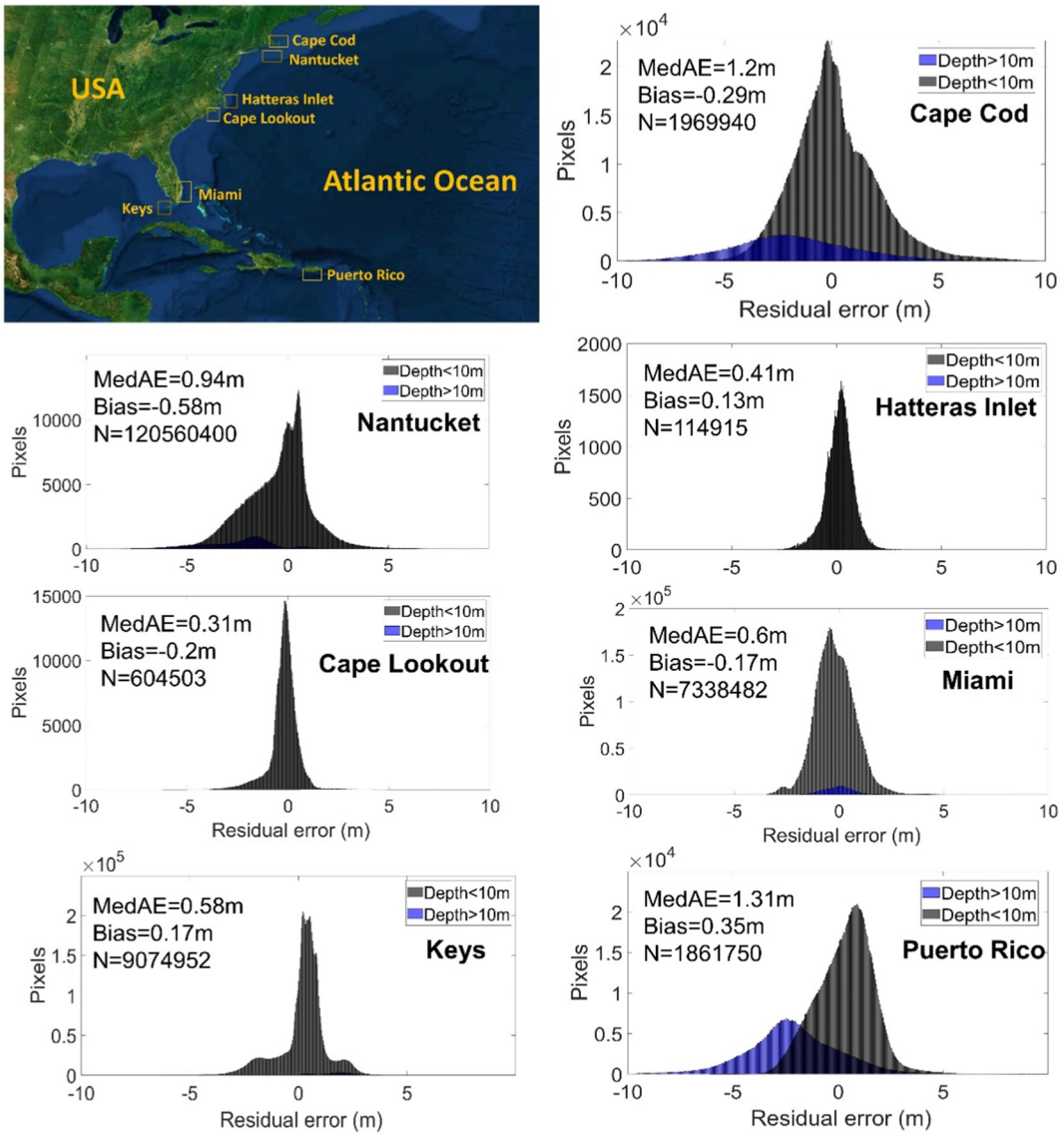

Fig. 2. Location of the study regions in Puerto Rico, Florida Keys, Miami, Cape Lookout, Hatteras Inlet, Nantucket, and Cape Code showing the histograms of errors for the validation of satellite-derived bathymetry (SDB) with high-resolution in-situ lidar surveys.

(Table 1), following methods described in Caballero and Stumpf (2020a,b). The use of charts, which often do not include the most current soundings, may introduce some errors in the calibration but demonstrates the utility of the method without dependence on current high-resolution surveys. This procedure is significant for evaluating a precise approach that can be replicated in remote areas or regions without the requirement of high-resolution bathymetry. Using chart soundings also assures complete independence of the calibration data set from the validation lidar surveys. To test the robustness of the calibration using charts, the same approach has been applied in each of the seven study regions. For explicit information on the multi-scene methodological strategy, consult Caballero and Stumpf (2020a,b).

Table 1
Calibration with chart data (m_1 and m_{offset}) and accuracy statistics (MAE, MedAE, Bias, and N) of SDB against high-resolution lidar for each study region. The most complex areas corresponded to North Carolina and New England.

Region	m_1	m_{offset}	MAE (m)	MedAE (m)	Bias (m)	N
Cape Cod	85.2	0.868	1.50	1.20	−0.29	1,969,940
Nantucket	72.55	0.878	1.33	0.94	−0.58	120,560,400
Hatteras Inlet	90.84	0.949	0.51	0.41	0.13	114,915
Cape Lookout	68.0	0.944	0.48	0.31	−0.20	604,503
Keys	67.8	0.938	0.79	0.58	0.17	9,074,952
Miami	45.8	0.925	0.71	0.60	−0.17	7,338,482
Puerto Rico	47.1	0.877	1.42	1.31	0.35	1,861,750

2.4. Optically deep-water areas

As SDB continues to expand in the application, defining the limits of usable data becomes significant (Caballero and Stumpf, 2020a,b, 2021). A key component is the maximum detectable depth, namely the depth of optically deep water (ODW), where the seafloor is too deep for a bottom reflectance signal to be returned. Considering the variation in residual turbidity over the seven study regions, two criteria were applied to identify the location of water too deep for accurate depth retrievals. For the clearest water, we used a supervised threshold of $\leq 0.003\ sr^{-1}$ for the blue (490 nm) and green (560 nm) reflectance bands after the composite, with pixels having these values masked as ODW. These thresholds were chosen

after the inspection of histograms and values for optically deep and shallow pixels in the seven study sites. For water that was identified as optically shallow (reflectance above this threshold), we then applied an additional turbidity threshold. Caballero et al. (2019) calculated a relationship between the turbidity proxy (red-edge band, Rrs 704 nm) versus SDB for a time series:

$$\log\left(\mathrm{SDB}_{\mathrm{odw}}\right) = -0.251 * \log\left(\mathrm{Rrs704}\right) + 0.8. \quad (3)$$

The algorithm did not retrieve depths if the depth was greater than $\mathrm{SDB}_{\mathrm{odw}}$. Based on the Rrs704 of the composite image, ODW was defined as having values where the retrieved $\mathrm{SDB}_{\mathrm{odw}}$ was less than the retrieved SDB depth. If either criterion applies, the water is deemed optically deep. Over clear areas, where there is negligible turbidity, the first cutoff using both blue and green bands can mask out ODW, whereas, over moderately turbid areas, the second cutoff defines the maximum detectable depth. This approach is image based, automated, and broadly applicable, as it was tested in the seven study regions that have different water quality conditions and seabed habitats.

2.5. Validation with lidar data

The airborne lidar bathymetry (ALB) in the seven study regions was obtained from the National Geodetic Survey (NGS). These datasets were collected by the Joint Airborne Lidar Bathymetry Technical Center of Expertise (JALBTCX) in 2018 and 2019 using the Coastal Zone Mapping and Imaging Lidar (CZMIL) system. These Digital Elevation Models (DEMs) contained rasterized bathymetry at a 1-meter grid size. Anomalous high and low elevation values have been flagged and removed, and point cloud classification algorithms have been validated via manual review and QA/QC. Bathymetric lidar coverage extends from the shoreline to 1000 m offshore or to the range of the laser, which penetrates 2 to 3 times the Secchi Depth depending on environmental conditions. The vertical and horizontal accuracy of these datasets is 10 cm and 100 cm, respectively at a 95 % confidence level. The high-resolution ALB observations were selected as the reference in the study sites and compared to SDB products for validation and quality assessment. ALB datasets were subsequently gridded to the Sentinel-2's image resolution (10 m), averaging ALB points within each 10-m grid cell. To assess the accuracy of SDB retrieval with the multi-temporal SDB, Mean Absolute Error (MAE), Median Absolute Error (MedAE), and mean bias were calculated by comparing with the validation data for the entire depth range and within five-meter depth intervals for each study site.

3. Results

Seven study sites, having different atmospheric conditions, water quality, and benthic habitats, were selected along the Caribbean and the eastern coast of the U.S. (Figs. 1 and 2): in 2018 Puerto Rico and New England (Cape Cod and Nantucket), and in 2019 Florida (Miami and Keys) and North Carolina (Cape Lookout and Hatteras Inlet). Puerto Rico and Florida areas were chosen as representatives of more clear environments while the other featured more turbid environments. Sentinel-2 SDB maps that were calibrated with chart soundings were evaluated using extensive independent lidar sets in each study site. After ACOLITE atmospheric correction and the compositing approach, SDB retrieved depths with Median Absolute Error (MedAE) varying from 0.31 to 1.31 m (Fig. 2 and Table 1). In Puerto Rico, SDB retrieved information from 0 to 30 m (N = 1,861,750) with MAE of 1.42 m, MedAE of 1.31, and mean bias of 0.35 m. In Florida, bathymetry was obtained for the depth range of 0–25 m (N = 7,338,482) with Mean Absolute Error (MAE) of 0.71 m, MedAE of 0.60, and bias of −0.17 m over Miami and for the depth range of 0–15 m (N = 9,074,952) with MAE of 0.79 m, MedAE of 0.58, and bias of 0.17 m over the Florida Keys. In the most complex areas of North Carolina, SDB recovered data from 0 to 15 m (N = 604,503) with MAE of 0.48 m, MedAE of 0.31, and bias of −0.20 m over Cape Lookout and from 0 to 10 m (N = 114,915) with MAE of 0.51 m, MedAE of 0.41, and bias of 0.13 m over Hatteras Inlet. Finally, in Nantucket and Cape Cod, SDB retrieved information from 0 to 20 m with MAE of 1.33 m, MedAE of 0.94, and bias of −0.58 m (N = 120,560,400), and with MAE of 1.50 m, MedAE of 1.20 and bias of −0.29 m (N = 1,969,940), respectively. The clarity of the waters of Puerto Rico and Florida allowed mapping up to 30 m and 25 m, respectively, whereas the rest of the areas retrieved up to 15–20 m due to the less optimal environmental conditions. Generally, MedAE values were lower than 1 m, except in Puerto Rico and New England, and bias were lower than ±0.5 m. In Puerto Rico, higher errors resulted from a slight bias (underestimation) in deep waters (depths 10–30 m). The derived depths were plotted versus the lidar survey depths, demonstrating consistent patterns between SDB products and the validation data from shallow (<10 m) to deep (>10 m) waters (Fig. 1 Supplementary Information). A majority of the points in the scatterplots were distributed more densely along the 1:1 reference line, showing high accuracy. Hence, the proposed method produced SDB closest to the validation data. Comparing the histograms of residual errors and the scatterplots shows such a conclusion.

The MedAE and bias results at binned depths were inspected to further evaluate the stability of the model performance at different depth ranges, calculating the error metrics in shallow waters (0–5 m), medium depth

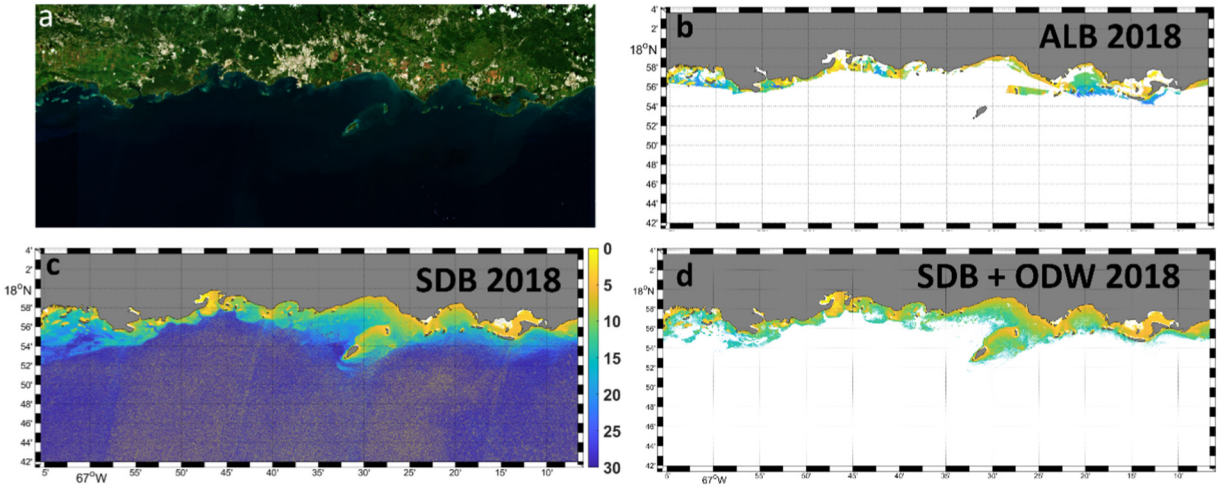

Fig. 3. a) RGB composite of Sentinel-2 in Puerto Rico, b) airborne lidar bathymetry (ALB) survey at 1 m spatial resolution in 2018, c) map of SDB at 10 m spatial resolution in 2018, and d) map of SDB after masking out optically-deep waters (ODW).

group (5–10 m), and deeper waters (10–15 m, 15–20 m, 20–25 m, 25–30 m) according to the lidar data (Fig. 2 Supplementary Information). SDB achieved higher errors with increased depth ranges, and the shallow and medium depths were more accurate than the deeper depths in all the study sites. SDB errors typically indicate a relationship with the water depth. The median errors increased sharply to >1–2 m at the depth range of 20–30 m; effectively error is proportional to depth. In addition, bias was negative for all sites and depths >10 m, except in Florida, indicating a general underestimation of SDB over deep areas. The capability of SDB detection was constrained to maximum depths of around 20 m. Nonetheless, shallow depths exhibited a significantly consistent decrease of the error down to the 0–5 m increment with an overall MedAE <0.5 m.

Depth maps of SDB at 10 m (Figs. 3–9c–d) and airborne lidar at 1 m (Figs. 3–9b) are displayed in the seven study sites (Figs. 3–9a), indicating coherent spatial patterns from shallow to deep waters. SDB is consistent with lidar surveys on many details of the seabed geomorphology. For instance, in bays (like Biscayne), similar bathymetric features (reef structures,

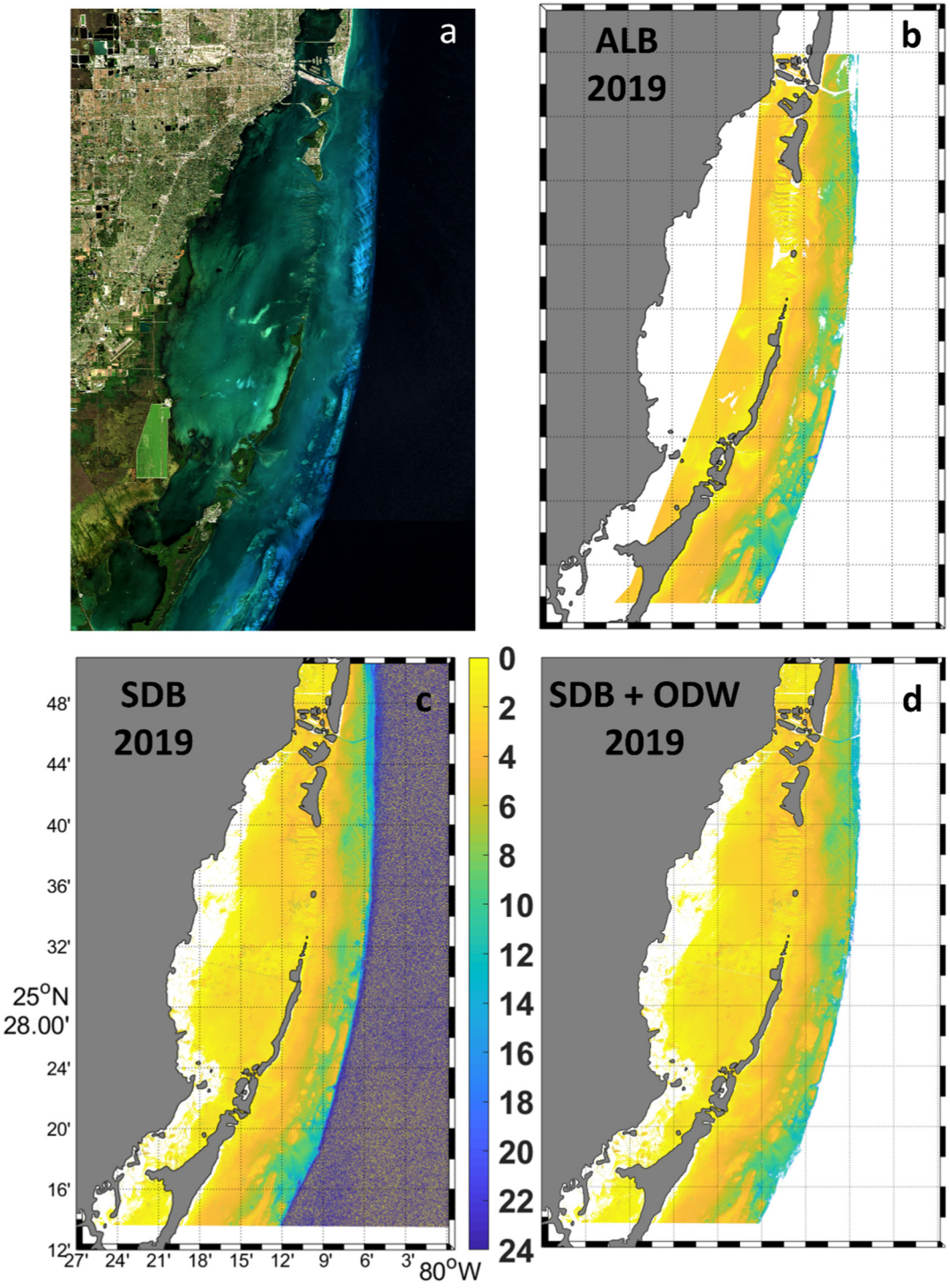

Fig. 4. a) RGB composite of Sentinel-2 in Miami area, including Biscayne Bay, b) airborne lidar bathymetry (ALB) survey at 1 m spatial resolution in 2019, c) map of the final SDB at 10 m spatial resolution in 2019, and d) map of the final SDB after masking out optically-deep waters (ODW).

channels into Biscayne Bay, etc.) can be observed with both instruments from shallow to offshore deep waters (Fig. 4). Moreover, SDB allowed mapping the shelf boundary, in particular where the reef shelf drops to the offshore ocean, as could be observed in Puerto Rico (Fig. 3) or the Florida Keys (Fig. 8). SDB shows topographical details from the shallow regions to areas up to 20–30 m. It is worth mentioning that coverage is more sparsely distributed for the lidar surveys compared to SDB; the SDB spanned a more extended area than lidar, indicating depths >15 m, beyond the slope into the ODW. For example, in Cape Lookout, Hatteras Inlet, and Nantucket, the satellite bathymetry results improved coverage in both the shallow and deeper coastal water. The composite SDB yields greater spatial coverage than lidar because it can retrieve data where the lidar mission may have been constrained by turbidity, surf, or logistical limitations on the extent of the survey.

Fig. 3 Supplementary Information shows the turbidity proxy of the red-edge band (remote sensing reflectance at 704 nm, Rrs 704) after the composite associated with the final SDB maps for each study site (Figs. 3–9c–d). Rrs 704 captures scattering, but it may also show a return from white sand in up to 3 m of water. While compositing reduces turbidity, some residual remains dependent on the overall water clarity conditions. On one hand, over clear environments such as Puerto Rico (and the reefs off Florida), minimum turbidity levels were associated with the composite. On the other hand, residual turbidity levels were encountered in North Carolina and New England, in particular, in Hatteras Inlet. The multi-temporal approach returns turbidity products indicating areas that may still have a residual shoaling bias or where the water is chronically optically deep due to severe turbidity. The SDB maps derived from the Sentinel-2 scenes were grainy over the ODW areas (Figs. 3–9c) and the noisy fluctuation of water depth was reflected in some offshore regions even with the filtering applied. However, ODW detection using the definition of the maximum detectable depth developed in this study, eliminated most of these artifacts (Figs. 3–9d), as well as otherwise invalid depth retrievals in water that is too deep or turbid to detect the bottom. The image-based masking for ODW was not tuned for these areas, indicating it is broadly applicable (Fig. 3 Supplementary Information).

4. Discussion and concluding remarks

4.1. Turbidity in satellite-derived bathymetry

The heterogeneity of the coastal environment generally deteriorates SDB performance, with turbid pixels producing underestimations in depths as already demonstrated in previous studies (Minghelli-Roman and Dupouy, 2013; Hamylton et al., 2015; Pe'eri et al., 2016; Caballero et al., 2019; Caballero and Stumpf, 2020a; Casal et al., 2020). To ensure accuracy and stability, especially over moderately turbid environments, correction for turbidity is necessary (Kutser et al., 2020; Ashphaq et al., 2021, Cesbron et al., 2021). By the compositing adjustment, SDB substantially enhances existing survey methods addressing the SDB algorithmic challenges faced by individual scene models. The multi-scene compositing strategy addressed limitations inherent in conventional methods, retrieving more data and pushing the method into the water with real and variable turbidity. Visual selection of a single "optimal" scene cannot accomplish this, because of the spatial and temporal heterogeneity of turbidity patterns (Caballero and Stumpf, 2020a). The approach carried out in the seven study regions from the Caribbean to New England indicated the compositing algorithm effectively estimated depth with a MedAE ranging from 0.31 to 1.31 m for depth ranges of 0–30 m. Bias results ranged from −0.58 to 0.35 m within

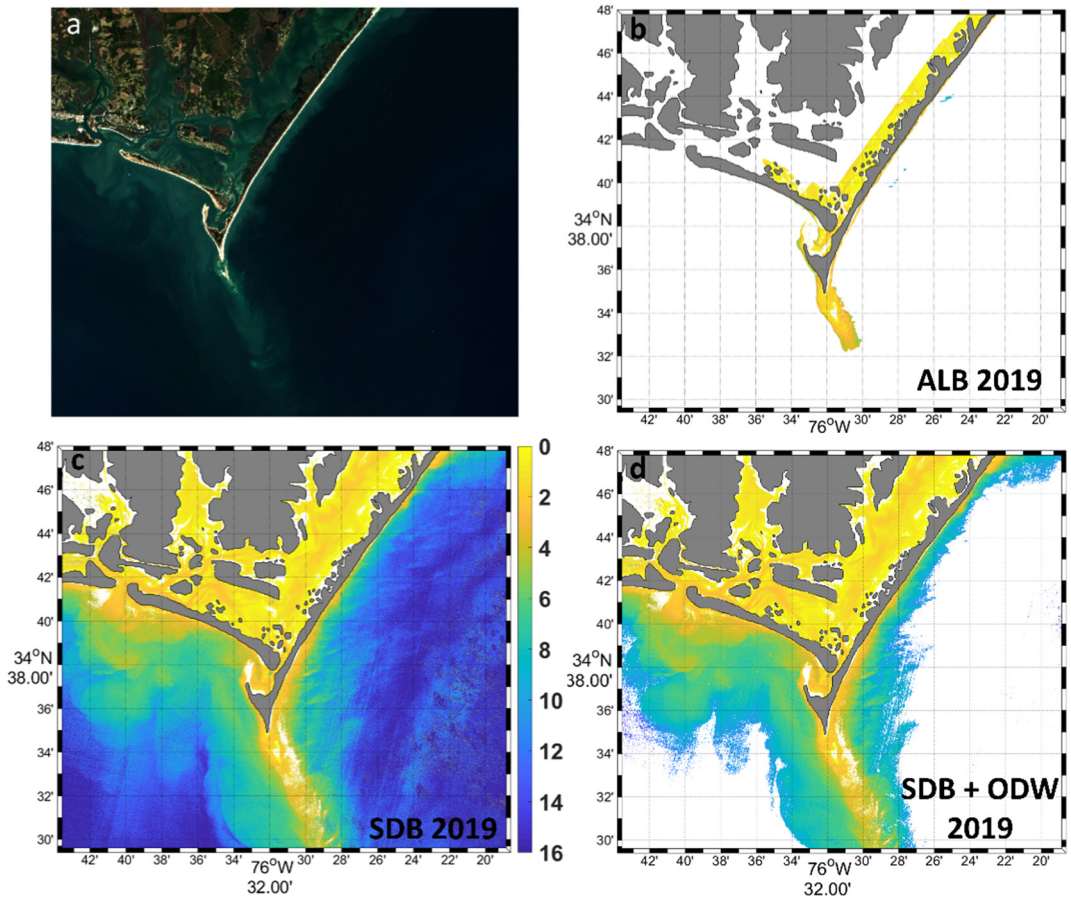

Fig. 5. a) RGB composite of Sentinel-2 in North Carolina, b) airborne lidar bathymetry (ALB) survey at 1 m spatial resolution in 2019, c) map of the final SDB at 10 m spatial resolution in 2019, and d) map of the final SDB after masking out optically-deep waters (ODW).

the different study sites, results that could be ascribed to areas being heterogeneous in water constituent compared to recent SDB findings obtained over coral reefs and clear water environments (Hedley et al., 2018; Evagorou et al., 2019; Li et al., 2019; Poursanidis et al., 2019; Sagawa et al., 2019). These outcomes show that multi-temporal compositing provides a capability that makes progress in detecting SDB in environments from clear water to water with residual turbidity.

The calibrations (Table 1 in Methods) showed a consistent change in slope (m_1, Eq. (2), see Methods) from lower values in clear water (Miami and Puerto Rico) to higher values in areas with consistent turbidity (Nantucket, Cape Cod, and Hatteras). Caballero and Stumpf (2020a,b) transferred calibrations between clear and turbid water areas and got similar error metrics. There is an assumption that empirical coefficients vary randomly, thereby necessitating extensive tuning. These results suggest this is not the case, and that there is a consistency in the behavior of the two coefficients. The m_1 appears to depend on turbidity; potentially the calibration can be adjusted based on the background turbidity to achieve a reasonable first estimate. The m_{offset} coefficient relates the relative SDB (pSDB in Methods) to the reference datum. The similarity in m_{offset} values across regions suggests that it may be possible to converge on a standard value for m_{offset}, particularly once the influence of water level (tide) on the values is addressed (as tides will inherently alter the relationship of "zero" depth in the SDB to the reference datum).

Accuracy does vary between depths. The bathymetry errors of all the sites showed a declining error with decreased depth (Fig. 2 Supplementary Information). Overall, all show the same trend in MedAE; when depths >15 m were retrievable, the model slightly underestimated (negative bias) the depth. This may reflect a lack of signal from lower albedo substrates. Ultimately, even in the clearest water, the water column completely attenuates the light reflected from the bottom (Dekker et al., 2011). The maximum retrievable depth in these cases (over bright substrates) appears to be about 30 m. Otherwise, SDB performed best in the 0–15 m range. Similar findings with severe underestimation for depths in the range of 10–20 m were found in other studies (Kerr and Purkis, 2018; Traganos et al., 2018; Caballero and Stumpf, 2019; Geyman and Maloof, 2019; Susa, 2022). Different benthic surfaces with variable bottom reflectance are located in each of the study sites (e.g., sand, reef, deep coral, seagrass, and rocks). While substrate albedo may limit the maximum retrievable depth, our results suggest that benthic substrates are not otherwise a source of error as initially demonstrated in Stumpf et al. (2003) and subsequent papers (Caballero and Stumpf, 2019; Caballero et al., 2019; Caballero and Stumpf, 2020a,b, 2021).

Traditionally, imagery for SDB is analyzed to eliminate artifacts from turbidity, waves, and clouds. In this study, images were only screened to remove those with cloud cover, as the compositing method addressed the other artifacts. Previous research suggested that machine-learning models are more affected by environmental variables than the inversion models with empirical calibration, as the one used in this study (Kibele and Shears, 2016; Duan et al., 2022). Li et al. (2019) applied the band-ratio algorithm (Stumpf et al., 2003) for depth retrieval and generated a manually selected water attenuation index for pristine viewing conditions in offshore waters, which may not always represent the water attenuation conditions in shallow areas. On the other hand, SDB for single images was improved by estimating the inherent optical properties and using tuning coefficients (Kerr and Purkis, 2018; Zhu et al., 2020). Our compositing approach automatically accounted for turbidity conditions, as well as incorporated sunglint correction and gaps reduction. These advances are key; the SDB model is more widely applicable to a variety of environments from clear (the Caribbean), moderately turbid (Florida Keys and Miami) to severely turbid (North Carolina and New England) areas.

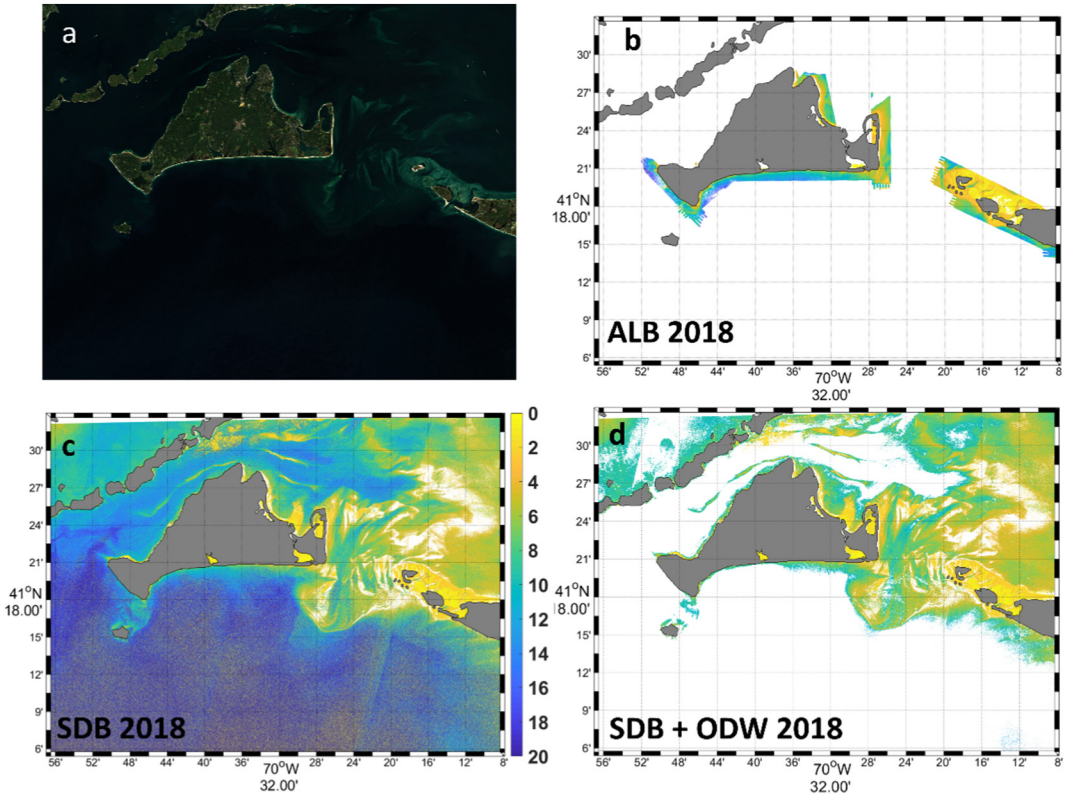

Fig. 6. a) RGB composite of Sentinel-2 in Nantucket, b) airborne lidar bathymetry (ALB) survey at 1 m spatial resolution in 2018, c) map of the final SDB at 10 m spatial resolution in 2018, and d) map of the final SDB after masking out optically-deep waters (ODW).

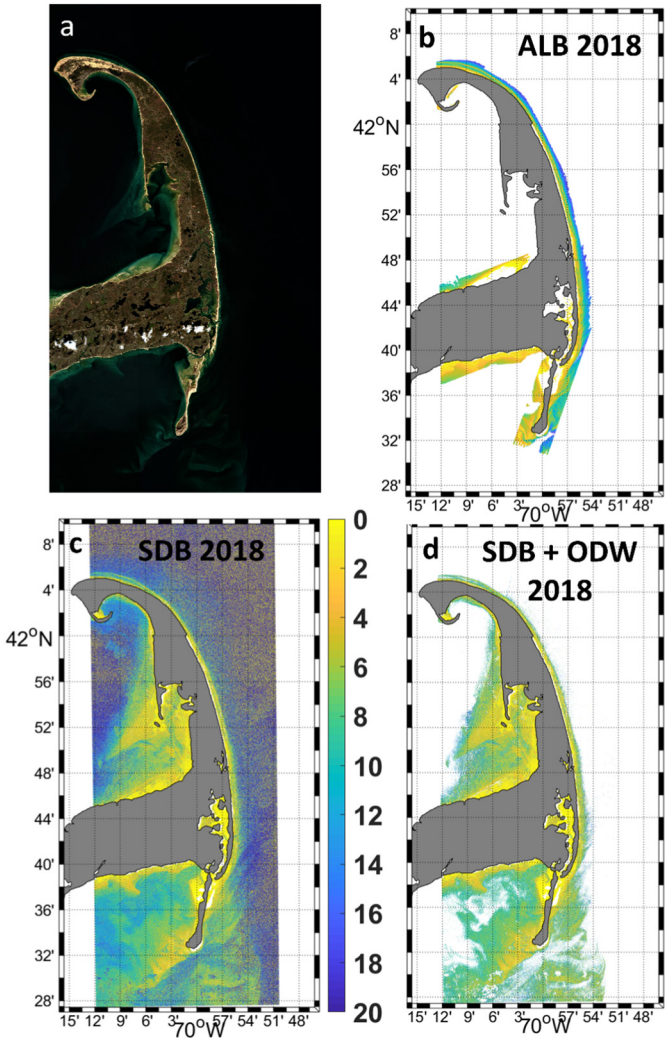

Fig. 7. a) RGB composite of Sentinel-2 in Cape Cod, b) airborne lidar bathymetry (ALB) survey at 1 m spatial resolution in 2018, c) map of the final SDB at 10 m spatial resolution in 2018, and d) map of the final SDB after masking out optically-deep waters (ODW).

4.2. Optically deep-water masking

ODW is important information, given the depth constraints of SDB, but is typically inferred by interpretation of SDB imagery, rather than delineated (Lee et al., 2022). Methods for determining ODW are new and focus mainly on clear water environments. Lee et al. (2022) used a supervised threshold of spectral and band ratio analysis in the Bahamas, Tanzania, and the Wadden Sea. Cao et al. (2020) implemented an empirical bathymetric retrieval method to exclude non-optimal image data from the image on a per-pixel basis. Other advances in the estimation of chlorophyll-a concentration from optical imagery accounted for inherent optical properties by refining algorithms to automate the identification of ODW (McCarthy et al., 2022). Lee et al. (2021) developed a prototype confidence score system obtained through the fusion of lidar and Landsat-8 data in the Bahamas, a clear water site, which eliminates ODW and classifies all pixels of optically shallow waters into three categories with a preliminary set of criteria. A regional high-resolution bathymetry of the North West Shelf of Australia based on Sentinel-2 satellite images was lately accomplished using Stumpf et al. (2003) SDB model, where the maximum depth of validity of the data was delineated by using a threshold coefficient of correlation between SDB and the calibration data (Lebrec et al., 2021).

Using a small set of optically-based rules, we developed an automated model for masking ODW and defining the maximum detectable depth that can be applied in both clear and turbid water. This study showed that the ODW mask can eliminate large areas of data that would be invalid (Figs. 3–9). The criteria in our method apply conditions suitable for clear water (masking pixels with blue or green bands ≤ 0.003 sr^{-1}, see Methods) and turbid water using a turbidity proxy solution from Caballero et al. (2019) (Eq. (3) in Methods). This approach allows transferability to other environments with no tuning requirement. However, refinement of the ODW method is still needed in areas of chronic moderate turbidity. A comparison of Fig. 6d with NOAA chart data 13,241 (https://charts.noaa.gov/OnLineViewer/13241.shtml) indicated some invalid shallow values for ODW over Nantucket Sound north of Nantucket (41° 24′ N and 70° 16′W), the most complex region evaluated here. These might have resulted from high and constant turbidity patterns in all the multi-temporal scenes used in the composite. The ODW solution may require adjustment to address these severe and chronic turbid environments. Further research will be necessary to understand what factors caused the ODW solution to miss the chronically turbid features in this site. In other cases, the masking excluded most ODW problematic areas (Figs. 3–9).

4.3. Sentinel-2 in support of shallow coastal bathymetry for global science applications

The multi-temporal strategy can provide effective depths in a range of environments from near tropical to temperate moderately turbid waters (Figs. 2–3 Supplementary Information). Defined relationships between depth limitation and turbidity are needed to identify ODW, thereby improving the resulting bathymetric maps. This approach allows for an automated detection that does not depend on the local tuning of a model for ODW. Inconsistencies in the composite could be expected where merging scenes are collected at substantially different times, such as before and after extreme weather events, or over several years. We recommend implementing the multi-temporal model with a maximum temporal range of 6 months, depending on the application case. In addition, a new Specification Matrix has been introduced in the 6th S-44 Edition of the International Hydrographic Organization's Standards for Hydrographic Surveys (International Hydrographic Organization-IHO, 2020), which added flexibility for other types of hydrographic surveys carried out for purposes beyond the safety of navigation. Our outcomes (Fig. 2; Figs. 1–2 Supplementary Information) are in accordance with the S-44 Matrix code, reporting a total vertical uncertainty (TVU) generally meeting Criteria 7 (Bc7 = 1 m) and Criteria 8 (Bc8 = 0.5 m) for depths <10 m and Criteria 6 (Bc6 = 2 m) and Criteria 7 (Bc7 = 1 m) for depths ≥10 m. This new standard provides a range of selectable criteria for bathymetric parameters as part of a hydrographic survey to allow flexibility and customization in the tasking and assessing of hydrographic surveys and the accommodation of new and emerging technologies, such as the assessment and characterization of SDB surveys. Notwithstanding, the generalization potential of the compositing model in a larger region still requires additional investigation, in particular, the tidal correction over meso- and macrotidal regime systems.

With the advancement of high spatial resolution satellite sensor technologies, SDB is becoming a powerful tool for deriving water depth in coastal waters. In addition, the photon-counting lidar system, Advanced Topographic Laser Altimeter System (ATLAS) onboard the Ice, Cloud, and land Elevation Satellite-2 (ICESat-2), launched on 15 September 2018 by NASA, can retrieve valuable bathymetry in shallow coastal and inland water body areas. Therefore, bottom-depth fusion from ICESat-2 and multispectral satellite imagery will be highly complementary, since ATLAS could potentially provide useful reference data for calibration (replacing soundings from nautical charts) for Sentinel-derived bathymetry in remote or poorly mapped areas. Consequently, this emerging information will ultimately enhance the effectiveness and competitiveness of SDB for coastal bathymetric products. The workflow presented in this study generated SDB maps that can be readily applied elsewhere in the U.S. and worldwide, encompassing a much larger range of time and spatial scales than using

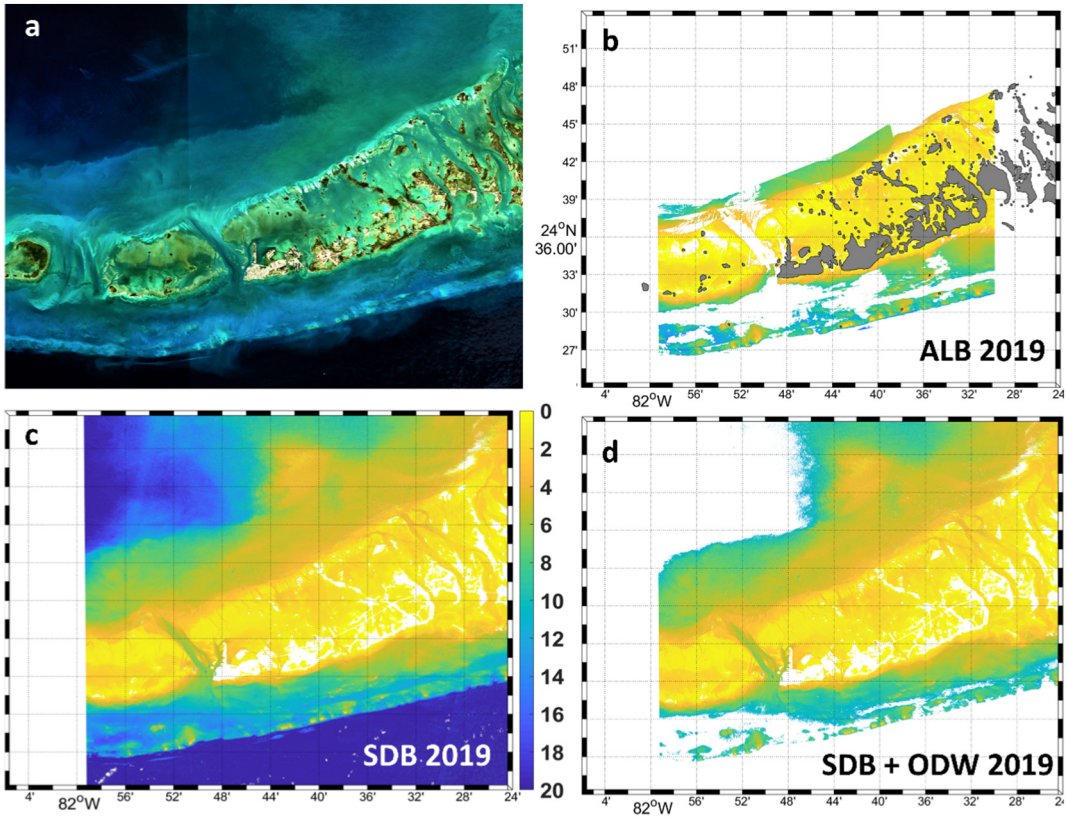

Fig. 8. a) RGB composite of Sentinel-2 in the Keys, b) airborne lidar bathymetry (ALB) survey at 1 m spatial resolution in 2019, c) map of the final SDB at 10 m spatial resolution in 2019, and d) map of the final SDB after masking out optically-deep waters (ODW).

field surveys. These methods can produce a consistent bathymetric product across different conditions, thereby supporting cost-effective routine bathymetric mapping of optically shallow waters. The promising approaches can be immediately applied in more environments with valuable implications to advance marine research, assess global vulnerabilities, and climate change impacts in coastal ecosystems, and assist management, monitoring, industry, and navigation. This information allows low-cost and scalable alternatives to field monitoring and can be applied to identify coastal features with high spatial detail. A practical example is the characterization of hurricane-induced bathymetric changes in the U.S. (Caballero and Stumpf, 2021; Herrmann et al., 2022). As a result, SDB may substantially enhance change detection and support recursive coastal monitoring. Moreover, SDB maps at this resolution can describe geomorphic features, which can advance benthic habitat monitoring and classification (Hedley et al., 2018; Kutser et al., 2020). In this regard, it is indispensable to mention the Nippon Foundation-GEBCO Seabed 2030 project, which can be almost entirely fulfilled by improved SDB methodologies such as the ones developed in this study. With routine and repetitive image acquisition, the Sentinel-2 mission can generate information supporting the onset of research projects at local, regional, and national scales for historical, contemporary, and quasi-real-time seabed monitoring.

CRediT authorship contribution statement

I. Caballero conceived and designed the research, collected the satellite data, processed the imagery, and conducted the analysis. I. Caballero led the writing of the manuscript with revision from R. P. Stumpf.

Data availability

Satellite-derived bathymetry data that support the findings of this study can be provided upon request. Airborne lidar bathymetry can be downloaded from https://coast.noaa.gov/dataviewer/#/lidar/search/. Chart data can be downloaded from https://www.charts.noaa.gov/. The Sentinel-2 Level-1C products were downloaded from the Copernicus Open Access Hub.

Declaration of competing interest

The authors declare that they have no known competing financial interests or personal relationships that could have appeared to influence the work reported in this paper.

Acknowledgments

This research was funded by grants RTI2018-098784-J-I00 (Sen2Coast Project) and IJC2019-039382-I (Juan de la Cierva-Incorporación) funded by MCIN/AEI/10.13039/501100011033 and by "ERDF A way of making Europe". The research was also supported by the National Oceanic and Atmospheric Administration (NOAA), National Geodetic Survey. We thank the European Space Agency, the European Commission, and the Copernicus program for distributing Sentinel-2 imagery. Thanks to the Joint Airborne Lidar Bathymetry Technical Center of eXpertise (JALBTCX), the National Oceanic and Atmospheric Administration (NOAA), and the National Geodetic Survey (NGS) for providing the valuable high-resolution lidar surveys used for this study. This work represents a contribution to CSIC Thematic Interdisciplinary Platform PTI TELEDETECT.

Appendix A. Supplementary data

Supplementary data to this article can be found online at https://doi.org/10.1016/j.scitotenv.2023.161898.

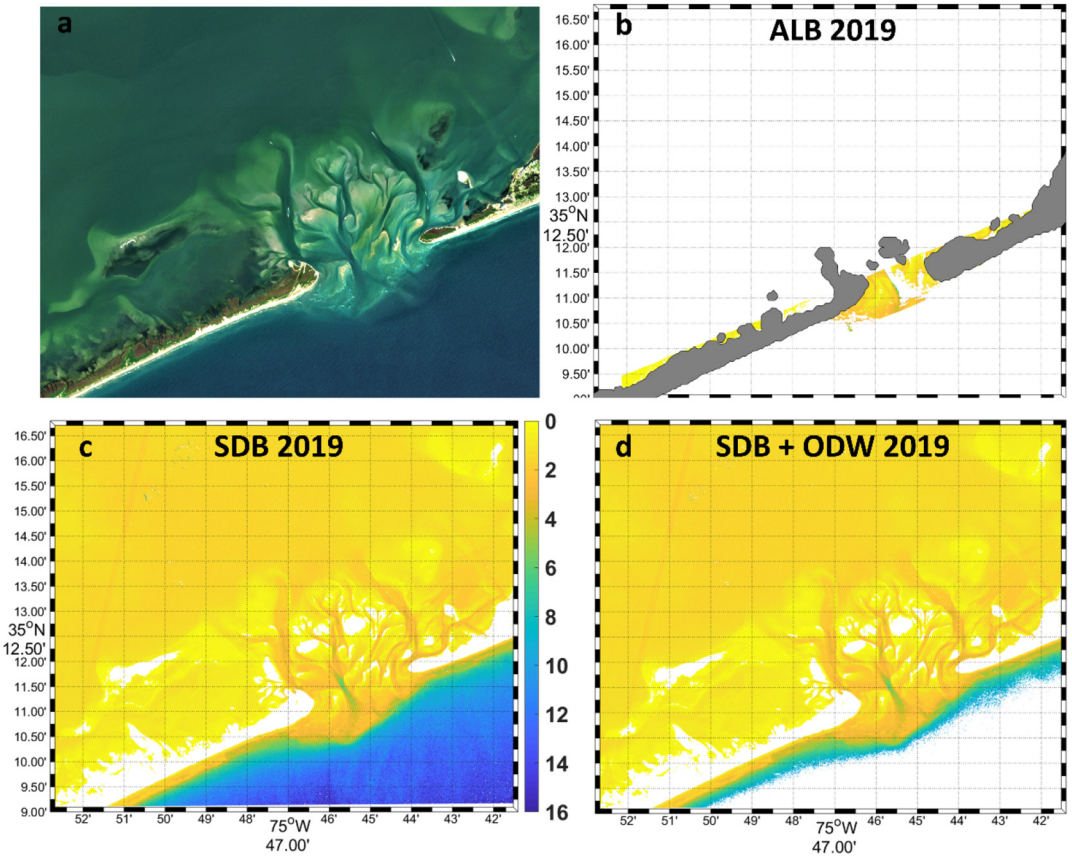

Fig. 9. a) RGB composite of Sentinel-2 in Hatteras Inlet, b) airborne lidar bathymetry (ALB) survey at 1 m spatial resolution in 2019, c) map of the final SDB at 10 m spatial resolution in 2019, and d) map of the final SDB after masking out optically-deep waters (ODW).

References

Ashphaq, M., Srivastava, P.K., Mitra, D., 2021. Review of near-shore satellite derived bathymetry: classification and account of five decades of coastal bathymetry research. J. Ocean Eng. Sci 6 (4), 340–359. https://doi.org/10.1016/j.joes.2021.02.006.

Beck, M.W., Losada, I.J., Menéndez, P., Reguero, B.G., Díaz-Simal, P., Fernández, F., 2018. The global flood protection savings provided by coral reefs. Nat. Commun. 9 (1), 1–9. https://doi.org/10.1038/s41467-018-04568-z.

Bergsma, E.W., Almar, R., 2020. Coastal coverage of ESA'Sentinel 2 mission. Adv. Space Res. 65 (11), 2636–2644. https://doi.org/10.1016/j.asr.2020.03.001.

Biermann, L., Clewley, D., Martinez-Vicente, V., Topouzelis, K., 2020. Finding plastic patches in coastal waters using optical satellite data. Sci. Rep. 10 (1), 1–10. https://doi.org/10.1038/s41598-020-62298-z.

Caballero, I., Stumpf, R.P., 2019. Retrieval of nearshore bathymetry from sentinel-2A and 2B satellites in South Florida coastal waters. Estuar. Coast. Shelf Sci. 226, 106277. https://doi.org/10.1016/j.ecss.2019.106277.

Caballero, I., Stumpf, R.P., 2020. Towards routine mapping of shallow bathymetry in environments with variable turbidity: contribution of sentinel-2A/B satellites mission. Remote Sens. 12 (3), 451. https://doi.org/10.3390/rs12030451.

Caballero, I., Stumpf, R.P., 2020. Atmospheric correction for satellite-derived bathymetry in the Caribbean waters: from a single image to multi-temporal approaches using sentinel-2A/B. Opt. Express 28 (8), 11742–11766. https://doi.org/10.1364/OE.390316.

Caballero, I., Stumpf, R.P., 2021. On the use of Sentinel-2 satellites and lidar surveys for the change detection of shallow bathymetry: the case study of North Carolina inlets. Coast. Eng. 169, 103936. https://doi.org/10.1016/j.coastaleng.2021.103936.

Caballero, I., Stumpf, R.P., Meredith, A., 2019. Preliminary assessment of turbidity and chlorophyll impact on bathymetry derived from sentinel-2A and sentinel-3A satellites in South Florida. Remote Sens. 11 (6), 645. https://doi.org/10.3390/rs11060645.

Caballero, I., Fernández, R., Escalante, O.M., Mamán, L., Navarro, G., 2020. New capabilities of sentinel-2A/B satellites combined with in situ data for monitoring small harmful algal blooms in complex coastal waters. Sci. Rep. 10 (1), 1–14. https://doi.org/10.1038/s41598-020-65600-1.

Cao, B., Deng, R., Zhu, S., Liu, Y., Liang, Y., Xiong, L., 2020. Bathymetric retrieval selectively using multiangular high-spatial-resolution satellite imagery. IEEE J. Sel. Top. Appl. Earth Obs. Remote Sens. 14, 1060–1074. https://doi.org/10.1109/JSTARS.2020.3040186.

Casal, G., Harris, P., Monteys, X., Hedley, J., Cahalane, C., McCarthy, T., 2020. Understanding satellite-derived bathymetry using sentinel 2 imagery and spatial prediction models. GIsci. Remote Sens. 57 (3), 271–286. https://doi.org/10.1080/15481603.2019.1685198.

Cesbron, G., Melet, A., Almar, R., Lifermann, A., Tullot, D., Crosnier, L., 2021. Pan-European satellite-derived coastal bathymetry-review, user needs and future services. Front. Mar. Sci. 1591. https://doi.org/10.3389/fmars.2021.740830.

Cira, M., Bafna, A., Lee, C.M., Kong, Y., Holt, B., Ginger, L., Jay, J.A., 2022. Turbidity and fecal indicator bacteria in recreational marine waters increase following the 2018 Woolsey fire. Sci. Rep. 12 (1), 1–13. https://doi.org/10.1038/s41598-022-05945-x.

Dekker, A.G., Phinn, S.R., Anstee, J., Bissett, P., Brando, V.E., Casey, B., Roelfsema, C., 2011. Intercomparison of shallow water bathymetry, hydro-optics, and benthos mapping techniques in Australian and Caribbean coastal environments. Limnol. Oceanogr. Methods 9 (9), 396–425. https://doi.org/10.4319/lom.2011.9.396.

Duan, Z., Chu, S., Cheng, L., Ji, C., Li, M., Shen, W., 2022. Satellite-derived bathymetry using Landsat-8 and sentinel-2A images: assessment of atmospheric correction algorithms and depth derivation models in shallow waters. Opt. Express 30 (3), 3238–3261. https://doi.org/10.1364/OE.444557.

European Space Agency, 2015. Sentinel-2 User Handbook. ESA Standard Document Paris, France. https://sentinel.esa.int/documents/247904/685211/Sentinel-2_User_Handbook.

European Space Agency, 2017. Sentinel-2 MSI Technical Guide. https://earth.esa.int/web/sentinel/technicalguides/sentinel-2-msi.

Evagorou, E., Mettas, C., Agapiou, A., Themistocleous, K., Hadjimitsis, D., 2019. Bathymetric maps from multi-temporal analysis of Sentinel-2 data: the case study of Limassol, Cyprus. Adv. Geosci. 45, 397–407. https://doi.org/10.5194/adgeo-45-397-2019.

Geyman, E.C., Maloof, A.C., 2019. A simple method for extracting water depth from multispectral satellite imagery in regions of variable bottom type. Earth Space Sci. 6 (3), 527–537. https://doi.org/10.1029/2018EA000539.

Hamylton, S.M., Hedley, J.D., Beaman, R.J., 2015. Derivation of high-resolution bathymetry from multispectral satellite imagery: a comparison of empirical and optimisation methods through geographical error analysis. Remote Sens. 7 (12), 16257–16273. https://doi.org/10.3390/rs71215829.

Hedley, J.D., Roelfsema, C., Brando, V., Giardino, C., Kutser, T., Phinn, S., Koetz, B., 2018. Coral reef applications of Sentinel-2: coverage, characteristics, bathymetry and benthic mapping with comparison to landsat 8. Remote Sens. Environ. 216, 598–614. https://doi.org/10.1016/j.rse.2018.07.014.

Herrmann, J., Magruder, L.A., Markel, J., Parrish, C.E., 2022. Assessing the ability to quantify bathymetric change over time using solely satellite-based measurements. Remote Sens. 14 (5), 1232. https://doi.org/10.3390/rs14051232.

Hunt, J.E., Tappin, D.R., Watt, S.F.L., Susilohadi, S., Novellino, A., Ebmeier, S.K., Udrekh, U., 2021. Submarine landslide megablocks show half of Anak Krakatau island failed on December 22nd, 2018. Nat. Commun. 12 (1), 1–15. https://doi.org/10.1038/s41467-021-22610-5.

International Hydrographic Organization-IHO, 2020. Standards for Hydrographic Surveys of the International Hydrographic Organization, S-44 Edition 6.0.0.
International Hydrographic Organization-IHO C-55, 2021. Publication C-55 "Status of Hydrographic Surveying and Charting Worldwide. IHO, Monte Carlo.
Kendall, M.S., Buja, K., Menza, C., Battista, T., 2018. Where, what, when, and why is bottom mapping Needed? An on-line application to set priorities using expert opinion. Geosciences 8 (10), 379. https://doi.org/10.3390/geosciences8100379.
Kerr, J.M., Purkis, S., 2018. An algorithm for optically-deriving water depth from multispectral imagery in coral reef landscapes in the absence of ground-truth data. Remote Sens. Environ. 210, 307–324. https://doi.org/10.1016/j.rse.2018.03.024.
Kibele, J., Shears, N.T., 2016. Nonparametric empirical depth regression for bathymetric mapping in coastal waters. IEEE J. Sel. Top. Appl. Earth Obs. Remote Sens. 9 (11), 5130–5138. https://doi.org/10.1109/JSTARS.2016.2598152.
Kutser, T., Hedley, J., Giardino, C., Roelfsema, C., Brando, V.E., 2020. Remote sensing of shallow waters–A 50 year retrospective and future directions. Remote Sens. Environ. 240, 111619. https://doi.org/10.1016/j.rse.2019.111619.
Lacroix, P., Dehecq, A., Taipe, E., 2020. Irrigation-triggered landslides in a peruvian desert caused by modern intensive farming. Nat. Geosci. 13 (1), 56–60. https://doi.org/10.1038/s41561-019-0500-x.
Lebrec, U., Paumard, V., O'Leary, M.J., Lang, S.C., 2021. Towards a regional high-resolution bathymetry of the north west shelf of Australia based on Sentinel-2 satellite images, 3D seismic surveys, and historical datasets. Earth Syst. Sci. Data 13 (11), 5191–5212. https://doi.org/10.5194/essd-13-5191-2021.
Lee, C.B., Traganos, D., Reinartz, P., 2022. A simple cloud-native spectral transformation method to disentangle optically shallow and deep waters in Sentinel-2 images. Remote Sens. 14 (3), 590. https://doi.org/10.3390/rs14030590.
Lee, Z., Shangguan, M., Garcia, R.A., Lai, W., Lu, X., Wang, J., Yan, X., 2021. Confidence measure of the shallow-water bathymetry map obtained through the fusion of lidar and multiband image data. J. Remote Sens. 2021. https://doi.org/10.34133/2021/9841804.
Li, J., Knapp, D.E., Schill, S.R., Roelfsema, C., Phinn, S., Silman, M., Asner, G.P., 2019. Adaptive bathymetry estimation for shallow coastal waters using planet dove satellites. Remote Sens. Environ. 232, 111302. https://doi.org/10.1016/j.rse.2019.111302.
Lin, N., Emanuel, K., Oppenheimer, M., Vanmarcke, E., 2012. Physically based assessment of hurricane surge threat under climate change. Nat. Clim. Chang. 2 (6), 462–467. https://doi.org/10.1038/nclimate1389.
Luijendijk, A., Hagenaars, G., Ranasinghe, R., Baart, F., Donchyts, G., Aarninkhof, S., 2018. The state of the world's beaches. Sci. Rep. 8 (1), 1–11. https://doi.org/10.1038/s41598-018-24630-6.
McCarthy, M.J., Otis, D.B., Hughes, D., Muller-Karger, F.E., 2022. Automated high-resolution satellite-derived coastal bathymetry mapping. Int. J. Appl. Earth Obs. Geoinf. 107, 102693. https://doi.org/10.1016/j.jag.2022.102693.
Melet, A., Teatini, P., Le Cozannet, G., Jamet, C., Conversi, A., Benveniste, J., Almar, R., 2020. Earth observations for monitoring marine coastal hazards and their drivers. Surv. Geophys. 41 (6), 1489–1534. https://doi.org/10.1007/s10712-020-09594-5.
Minghelli-Roman, A., Dupouy, C., 2013. Influence of water column chlorophyll concentration on bathymetric estimations in the lagoon of New Caledonia, using several MERIS images. IEEE J. Sel. Top. Appl. Earth Obs. Remote Sens. 6 (2), 739–745. https://doi.org/10.1109/JSTARS.2013.2239260.
Neumann, B., Vafeidis, A.T., Zimmermann, J., Nicholls, R.J., 2015. Future coastal population growth and exposure to sea-level rise and coastal flooding-a global assessment. PloS one 10 (3), e0118571. https://doi.org/10.1371/journal.pone.0118571.
Normandeau, A., MacKillop, K., Macquarrie, M., Richards, C., Bourgault, D., Campbell, D.C., Clarke, J.H., 2021. Submarine landslides triggered by iceberg collision with the seafloor. Nat. Geosci. 14 (8), 599–605. https://doi.org/10.1038/s41561-021-00767-4.
Osadchiev, A.A., 2018. Small mountainous rivers generate high-frequency internal waves in coastal ocean. Sci. Rep. 8 (1), 1–8. https://doi.org/10.1038/s41598-018-35070-7.
Pahlevan, N., Mangin, A., Balasubramanian, S.V., Smith, B., Alikas, K., Arai, K., Warren, M., 2021. ACIX-aqua: a global assessment of atmospheric correction methods for Landsat-8 and Sentinel-2 over lakes, rivers, and coastal waters. Remote Sens. Environ. 258, 112366. https://doi.org/10.1016/j.rse.2021.112366.
Pe'eri, S., Madore, B., Nyberg, J., Snyder, L., Parrish, C., Smith, S., 2016. Identifying bathymetric differences over Alaska's north slope using a satellite-derived bathymetry multitemporal approach. J. Coast. Res. 76 (10076, 56–63. https://doi.org/10.2112/SI76-006.
Plank, S., Marchese, F., Genzano, N., Nolde, M., Martinis, S., 2020. The short life of the volcanic island new Late'iki (Tonga) analyzed by multi-sensor remote sensing data. Sci. Rep. 10 (1), 1–15. https://doi.org/10.1038/s41598-020-79261-7.
Poursanidis, D., Traganos, D., Reinartz, P., Chrysoulakis, N., 2019. On the use of Sentinel-2 for coastal habitat mapping and satellite-derived bathymetry estimation using downscaled coastal aerosol band. Int. J. Appl. Earth Obs. Geoinf. 80, 58–70. https://doi.org/10.1016/j.jag.2019.03.012.
Rajendran, S., Sadooni, F.N., Al-Kuwari, H.A.S., Oleg, A., Govil, H., Nasir, S., Vethamony, P., 2021. Monitoring oil spill in NorilskRussia using satellite data. Scientific Reports 11 (1), 1–20. https://doi.org/10.1038/s41598-021-83260-7.
Sagawa, T., Yamashita, Y., Okumura, T., Yamanokuchi, T., 2019. Satellite derived bathymetry using machine learning and multi-temporal satellite images. Remote Sens. 11 (10), 1155. https://doi.org/10.3390/rs11101155.
Stumpf, R.P., Holderied, K., Sinclair, M., 2003. Determination of water depth with high-resolution satellite imagery over variable bottom types. Limnol. Oceanogr. 48 (1part2), 547–556. https://doi.org/10.4319/lo.2003.48.1_part_2.0547.
Su, J., Friess, D.A., Gasparatos, A., 2021. A meta-analysis of the ecological and economic outcomes of mangrove restoration. Nat. Commun. 12 (1), 1–13. https://doi.org/10.1038/s41467-021-25349-1.
Susa, T., 2022. Satellite derived bathymetry with Sentinel-2 imagery: comparing traditional techniques with advanced methods and machine learning ensemble models. Mar. Geod. 1–27. https://doi.org/10.1080/01490419.2022.2064572.
Traganos, D., Poursanidis, D., Aggarwal, B., Chrysoulakis, N., Reinartz, P., 2018. Estimating satellite-derived bathymetry (SDB) with the google earth engine and sentinel-2. Remote Sens. 10 (6), 859. https://doi.org/10.3390/rs10060859.
Turner, I.L., Harley, M.D., Almar, R., Bergsma, E.W., 2021. Satellite optical imagery in coastal engineering. Coast. Eng. 167, 103919. https://doi.org/10.1016/j.coastaleng.2021.103919.
van Zelst, V., Dijkstra, J.T., van Wesenbeeck, B.K., Eilander, D., Morris, E.P., Winsemius, H.C., de Vries, M.B., 2021. Cutting the costs of coastal protection by integrating vegetation in flood defenses. Nat. Commun. 12 (1), 1–11. https://doi.org/10.1038/s41467-021-26887-4.
Vanhellemont, Q., 2019. Adaptation of the dark spectrum fitting atmospheric correction for aquatic applications of the landsat and Sentinel-2 archives. Remote Sens. Environ. 225, 175–192. https://doi.org/10.1016/j.rse.2019.03.010.
Vanhellemont, Q., Ruddick, K., 2016. Acolite for Sentinel-2: aquatic applications of MSI imagery. Proceedings of the 2016 ESA Living Planet Symposium, Prague, Czech Republic, pp. 9–13.
Vanhellemont, Q., Ruddick, K., 2018. Atmospheric correction of metre-scale optical satellite data for inland and coastal water applications. Remote Sens. Environ. 216, 586–597. https://doi.org/10.1016/j.rse.2018.07.015.
Vitousek, S., Barnard, P.L., Fletcher, C.H., Frazer, N., Erikson, L., Storlazzi, C.D., 2017. Doubling of coastal flooding frequency within decades due to sea-level rise. Sci. Rep. 7 (1), 1–9. https://doi.org/10.1038/s41598-017-01362-7.
Zhu, J., Hu, P., Zhao, L., Gao, L., Qi, J., Zhang, Y., Wang, R., 2020. Determine the stumpf 2003 model parameters for multispectral remote sensing shallow water bathymetry. J. Coast. Res. 102 (SI), 54–62. https://doi.org/10.2112/SI102-007.1.